World Academy of Science, Engineering and Technology
International Journal of Mechanical and Mechatronics Engineering
Vol:5, No:1, 2011

Effect of Shell Dimensions on Buckling Behavior and Entropy Generation of Thin Welded Shells

Sima Ziaee, Khosro Jafarpur

***Abstract*—**Among all mechanical joining processes, welding has been employed for its advantage in design flexibility, cost saving, reduced overall weight and enhanced structural performance. However, for structures made of relatively thin components, welding can introduce significant buckling distortion which causes loss of dimensional control, structural integrity and increased fabrication costs. Different parameters can affect buckling behavior of welded thin structures such as, heat input, welding sequence, dimension of structure. In this work, a 3-D thermo elastic-viscoplastic finite element analysis technique is applied to evaluate the effect of shell dimensions on buckling behavior and entropy generation of welded thin shells. Also, in the present work, the approximated longitudinal transient stresses which produced in each time step, is applied to the 3D-eigenvalue analysis to ratify predicted buckling time and corresponding eigenmode. Besides, the possibility of buckling prediction by entropy generation at each time is investigated and it is found that one can predict time of buckling with drawing entropy generation versus out of plane deformation. The results of finite element analysis show that the length, span and thickness of welded thin shells affect the number of local buckling, mode shape of global buckling and post-buckling behavior of welded thin shells.

***Keywords*—**Buckling behavior, Elastic viscoplastic model, Entropy generation, Finite element method, Shell dimensions.

I. Introduction

WELDING, among all mechanical joining processes, has been employed at an increasing rate for its advantage in design flexibility, cost saving, reduced overall weight and enhanced structural performance. However, welding induces various types of distortion such as bowing, angular, and rotational distortion [1]. To study the effect of welding on structure efficiency, and carry out efficient distortion mitigation techniques, a valid method for predicting welding distortion is necessary.

Nowadays, in order to achieve reduction overall weight and more controllable manufacturing, the use of thinner section components in fabricating large structures has been more common. However, for relatively thin structures, welding can introduce significant buckling distortion which causes loss of dimensional control, structural integrity and increased fabrication costs due to poor fit-up between panels. Then it is necessary to achieve a predictive analysis technique to determine the susceptibility of a particular design to buckling distortion.

Welding-induced buckling of thin walled structures has been investigated in great details in [2]-[4]. Ueda *et al*. [2] presented a methodology to determine the buckling behavior of plates by large deformation elastic finite element method (FEM) and employing inherent strain distributions. Dean D. and Hidekazu [5] developed a prediction method of welding distortion which combines thermo-elastic-plastic finite element method (FEM) and large deformation elastic FEM based on inherent strain theory and interface element method and demonstrated the usefulness of using the proposed elastic FEM through the prediction of welding distortion in the large thin plate panel structures. Michaleris *et al*. [3], [6], [7] developed a predictive buckling analysis technique for thin section panels, combining decoupled 2-D weld process simulations and 3-D eigenvalue buckling analysis. Schenk T. et al. [8] presented a computational framework for the modeling of buckling distortion due to gas metal arc welding. They showed that not only the distortion amplitude but also the buckling mode is mesh-dependent. Phase transformation and transformation plasticity have also been incorporated in the analysis as shown by recent developments [9]-[10]. Dean and Hidekazu [5] investigated the influences of heat input, welding procedure, welding sequence, thickness of plate, and spacing between the stiffeners on buckling inclination in thin plate panel structures. Ziaee *et al*. [11] studied the influence of external restraint and thickness on buckling behavior of thin welded shells. Their study showed suitable combination of external restraint and thickness may eliminate global buckling. Falahi *et al*. [12] employed generated entropy during welding to compare maximum value of residual stresses due to variation of different thermal parameters such as welding velocity, heat input, welding sequence, and preheating treatment. They found that one can used entropy generation as a simple and efficient tool to compare residual stresses quantitatively.

In this work, 3-D thermo elastic-viscoplastic finite element analysis technique is applied to evaluate the effect of shell dimensions on buckling behavior and entropy generation due to welding.

S. Ziaee is an assistant professor in mechanical department of Yasouj University, (corresponding author to provide phone: 098-9173034751; fax: 098-741-222711; e-mail: ziaee@ mail.yu.ac.ir).

Kh. Jafarpur, is an associated professor in mechanical school of Shiraz University (e-mail: kjafame@shirazu.ac.ir).

II. Welding Analysis

Welding is a coupled thermo-mechanical process and its mathematical modeling consists of the balance of internal energy and balance of momentum as well as satisfying initial and boundary conditions [13]. To simplify the welding simulation, it is computationally efficient to perform the thermal and mechanical analysis separately. Physically, it is assumed that changes in mechanical state do not cause a change in thermal state [11]. Computation of the temperature history during welding and subsequent cooling is completed first, and then this temperature field is applied to the mechanical model to perform residual stress analysis.

A. Mechanical model

Anand model is a simple set of constitutive equations for large, isotropic, visco-plastic deformations [13]-[14] that employes employs a single scalar as an internal variable to represent the averaged isotropic resistance to plastic flow and needs no explicit yield condition and no loading/unloading criterion [14]. The inelastic strain rate $\dot{E}^P$ for Anand model is defined by [13]-[14]:

$$\dot{\mathbf{E}}^P \equiv \tilde{\mathbf{E}}^P(\mathbf{S}, z_1) = \dot{\varepsilon}^P \frac{\mathbf{S}}{\|\mathbf{S}\|}$$

$$\dot{\varepsilon}^P = \tilde{\varepsilon}^P(\mathbf{S}, z_1) = A \exp\left(-\frac{Q}{R\theta}\right)\left[\sinh\left(\xi \frac{\|\mathbf{S}\|}{z_1}\right)\right]^{\frac{1}{m}} \quad (1)$$

where the constitutive function $\tilde{\varepsilon}^P$ was proposed by Anand [14]. The equations of the internal variable z_1 are given by [13]:

$$\dot{z}_1 = h_0\left[1 - \frac{z_1}{z^*}\right]^a \dot{\varepsilon}^P \qquad for \quad z_1 \le z^*$$

$$\dot{z}_1 = -h_0\left[\frac{z_1}{z^*} - 1\right]^a \dot{\varepsilon}^P \qquad for \quad z_1 \succ z^* \quad (2)$$

with the criterion number

$$z^* = \bar{z}\left[\frac{\dot{\varepsilon}^P}{A}\exp\left(-\frac{Q}{R\theta}\right)\right]^\eta \quad (3)$$

where $A, Q, \xi, m, z, h_0, a, \bar{z}$, and η are constants of Anand model and R is the Boltzman's constant. The material constants for Anand model, which are used in the present work, are listed in Table I.

B. Thermal model

Because of the small size of melted region (weld pool) the heat source model developed by "moving isotherm pool" is used in this research.

The applied heat is transferred to the other regions, by conducting through the solid materials and convection to the surroundings. During a short time in welding, the welded region remains red-colored and a portion of heat is also dissipated by radiation.

Welding time in this work is calculated by dividing the welder speed that is obtained from the practical welding characteristic data by the length of the welded region. The temperature dependent thermal properties of material were also incorporated into the model (Table II).

TABLE I
CONSTANTS OF ANAND'S VISCOPLASTIC MODEL FOR THE SELECTED MATERIAL [15]

Parameter	*Value*	*Unit*	*Meaning*
Z	36.5	Mpa	Initial value of deformation resistance
Q/R	$\frac{175.3}{8.314}$	$\frac{KJ/mole}{KJ/mole \circ K}$	$\frac{Activation\ energy}{Universal\ gas\ content}$
A	1.91e7	Sec^{-1}	Pre-exponential factor
ς	7	Dimension less	Multiplier of stress
M	0.23348	Dimension less	Strain rate sensitivity of stress
h_0	1115.6	Mpa	Hardening/softening constant
$\bar{Z}$	18.9	Mpa	Coefficient for deformation resistance saturation value
N	.07049	Dimension less	Strain rate sensitivity of saturation value
A	1.3	Dimension less	Strain rate sensitivity of hardening/softening

TABLEII
VARIATION OF MATERIAL THERMAL AND MECHANICAL PROPERTIES WITH TEMPERATURE

T (^{0}C)	***Thermal Conductivity k(W/m.K)***	***Specific Heat C_p(J/kg.K)***	***Coeff. of Thermal Expansion (10^{-6})***	***Youngs Modulus E(GPa)***
20	222	904	23.3	72
50	230	930	23.6	72
100	230	930	24	70
150	250	965	25	67
200	260	965	25	67
250	272	985	25	61.5
300	272	980	26	61.5
350	278	1040	26	53
400	278	1100	26	45
450	283	1100	26	45
500	285	1100	26	35
550	285	1100	26	35
600	320	1100	26	17
650	400	1100	26	10
700	400	1100	26	10

C. Finite Element Approximation

The finite element method for uncoupled thermo-mechanical problem is based on the Ritz's approximation of variational equation, i.e. the principle of virtual work and the balance of internal energy.

The combined global finite element equation for the uncoupled thermo-mechanical problem is expressed by

$$\begin{bmatrix} \mathbf{K}_u^n & \mathbf{K}_{u\theta}^n \\ \mathbf{0} & \frac{1}{\Delta t}\mathbf{C}^n + \mathbf{K}_\theta^n \end{bmatrix} \begin{bmatrix} \Delta\mathbf{u} \\ \Delta\theta \end{bmatrix}^i = \begin{bmatrix} \mathbf{R}_u^{n+1} \\ \mathbf{R}_\theta^{n+1} \end{bmatrix} - \begin{bmatrix} \mathbf{F}_u^{n+1} \\ \mathbf{F}_\theta^{n+1} \end{bmatrix}^{(i-1)} \quad (4)$$

where $\mathbf{K}_u^n$ is the stiffness matrix corresponding to mechanical effects, $\mathbf{K}_{u\theta}^n$ is the matrix which transforms thermal energy into mechanical one. The thermal stiffness $\mathbf{K}_\theta^n$ is the sum of stiffness matrix corresponding to conduction, the stiffness related to convection phenomena, and the stiffness associated with radiation effects. $\Delta\mathbf{u}|_{(i)}$ and $\Delta\theta|_i$ are the vector of displacement and temperature increments, respectively; $\mathbf{R}_u^{n+1}$ is the vector of externally applied nodal point loads, $\mathbf{F}_u^{n+1}|_{i-1}$ is the vector of nodal point forces equivalent to the internal stresses. $\mathbf{R}_\theta^{n+1}$ is the summation of vectors of nodal thermal loads correspond to the thermal boundary condition. $\mathbf{F}_\theta^{n+1}|_{i-1}$ is the vector of nodal thermal loads correspond to the internal heat flux through the body surface ∂V.

The matrixes in (4) are taken at the current, n+1, and previous, n, time steps and current, (i), and previous, (i-1) iterations at the current time step.

The nonlinear finite element system of equations is solved iteratively by Newton-Raphson scheme.

III. Three-Dimensional Eigenvalue Analysis

Based on the Ziaee's research [11], in present work, approximated longitudinal transient stresses which produced in each time step, is applied to 3D-eigenvalue analysis to ratify predicted buckling time and corresponding eigenmode [11]. In order to predict the second buckling possibility of welded shell in post buckling behavior, modeling of post buckling equilibrium path in 3D-eigenvalue analysis is necessary.

IV. Entropy Generation Due to Welding

Fallahi et al [12] formulated the rate of generated entropy due to welding as follow:

$$\dot{S}_{gen}^{m} = \int_V \frac{k}{T^2}(\nabla T)^2 \qquad (5)$$

where T is thermal distribution of weldments at time step m, V is total volume of weldments, k is thermal conductivity and $\dot{S}$ is rate of entropy generation at time step m.

V. Model Validation

To check the accuracy of the proposed method, a specimen was constructed with a length, width, radius and thickness of L=500, W= 500, R=1000, t= 1.5 mm, respectively. One side of shells was fixed and welding was started from the free side, opposite side with fixture. The experimental model is constructed of Al100 whose mechanical properties are listed in Table I.The experimental model is welded using TIG method. Welding parameters are given in Table III. The emphasis in the experimental part was to observe the behavior of welded shells during welding.

TABLE III
WELDING PARAMETERS

Voltage	*8-10 Volts*
Current	90 Amps
Travel speed (Average)	254mm/minute

Fig.1, Fig.2 and Fig.3 show the comparison between analytical and experimental shapes of welded shells before removing torch, after removing torch and removing restraint after cooling down the specimen, respectively.

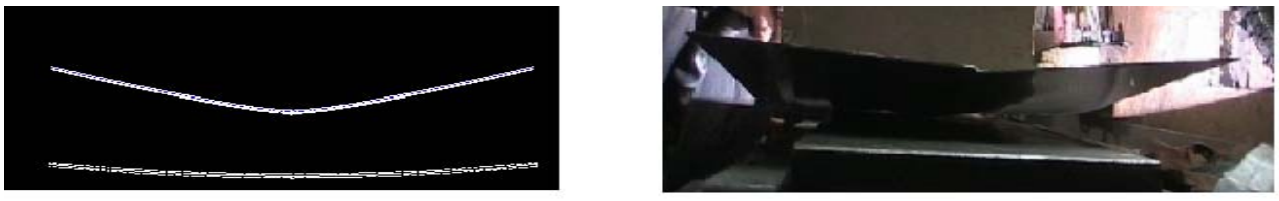

(a) Obtained by proposed FEM (b)Experiment

Fig.1 The front view of deformed welded shells exactly before removing torch

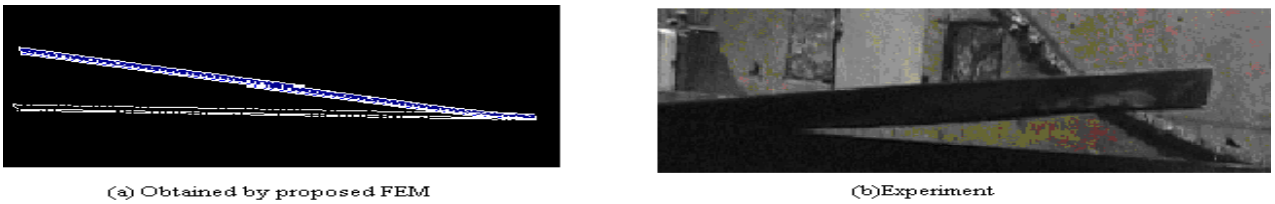

(a) Obtained by proposed FEM (b)Experiment

Fig. 2 The lateral view of deformed welded line exactly after removing torch

(a) Obtained by proposed FEM (b)Experiment

Fig.3: The front view of deformed welded shells after cooling down and removing the fixture

As these Figures illustrate, there is a good compatibility between the results. Therefore, the procedure presented here is suitable for estimating the behavior of specimen during welding.

VI. MODEL ANALYSIS

In this work, two thin wall shell sections are joined by a single pass butt welded. The radius of shells is assumed to be 1000mm and the length, the width, and the thickness of the shell varies. Fig. 4 shows dimensions of all studied cases. The line of welding is fixed in all models. The maximum number of elements that is used to construct the models are seven thousands 3D elements. Fine meshes are used near the weld line and with increasing distance from the weld line the mesh density is decreased. In order to obtain a highly precise prediction of welding distortion, material nonlinearity (thermo-viscoplastic) and geometrical nonlinearity (large deformation) are taken into account. However, uncoupled thermo-mechanical analysis is used to save computational time. The mechanical properties are dependent on the temperature history as listed in Table II.

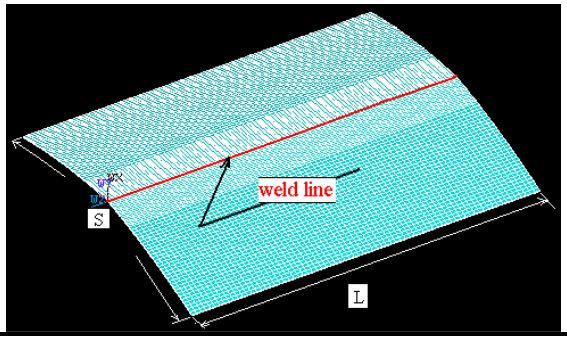

	Case 1	*Case 2*	*Case 3*	*Case 4*	*Case 5*
L (mm)	500	500	250	250	120
S (mm)	180	240	500	250	120
Thickness (mm)	1.5	1.5	1.5	1.5	1.5

Fig. 4: Dimension of studied cases.

VII. RESULTS ANF DISCUSSION

All cases experience sudden radial deformation (jumping) at the first buckling time and their equilibrium path from symmetrical behavior changed to asymmetrical one. After that, out of plain deformation enlarge increasingly and sometimes another jumping in radial deformation and new equilibrium path might be seen.

Table IV shows the influence of shell dimensions on buckling behavior due to welding. Based on it, cases 1 and 2 experience one clear global buckling during welding (Fig. 5a and 5b respectively) and local bucklings are not significant. In these cases, new deformation path gradually mutate into a newer one and before removing the torch, a jumping can be seen in this newer deformation without any change in the pattern of the deformation (Fig. 5c and 5d). It is found that this behavior can be classified in buckling after buckling. It is worth to mention that this can be confirmed by the use of eigenvalue analysis which employs the estimation of longitudinal stress as loading, in the post buckling path.

Cases 3 and 4 have two clear buckling time with different shapes during welding (Fig. 6b, 6c, 7a and 7b) and significant local bucklings which form near the weld line, around the moving torch and before the first global buckling (Fig. 6a). However, Case 5 dose not experience any buckling. In Table 4, the total entropy generated during a complete welding and the most radial deformation is also listed. As it expected, the total entropy generation is risen by increasing the weld line or the span of weldments. Also, it can be seen that as the total entropy increases, the radial deformation increases as well.

TABLE IV
EFFECT OF SHELL DIMENSIONS ON THE KIND, THE NUMBER OF BUCKLING AND THE VALUE OF TOTAL ENTROPY GENERATION

	Local Buckling (L.B.)	*Clear Global Buckling (G.B.)*	*Max. radial Deformation (mm)*	*Total Antropy Generation*
Case 1	No	One	21.9	79.04
Case 2	No	One	25.8	92.2
Case 3	Yes/ Especially Until Befor First G.B.	Two	20.6	52.55
Case 4	Yes/ Especially Until Befor First G.B.	Two	12.9	42.35
Case 5	No	No	1.4	16.23

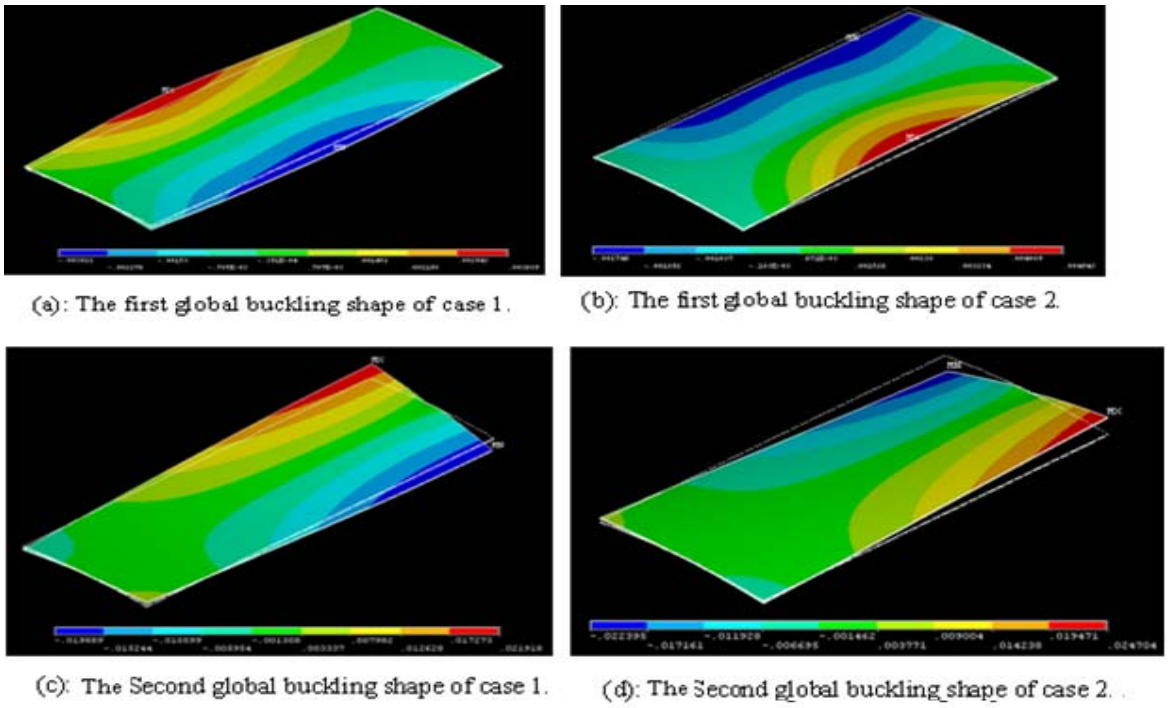

Fig. 5: Difference between global buckling of cases 1 and 2

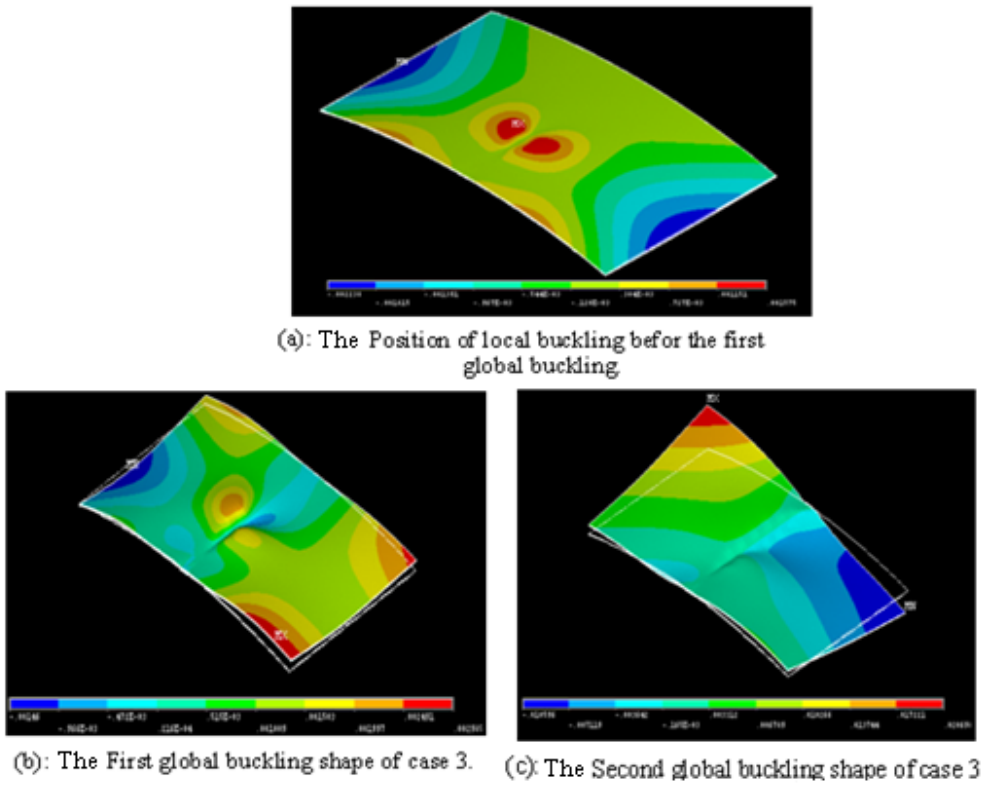

Fig. 6 Shape deformation of case 3 before and at the first global buckling and at the second global buckling

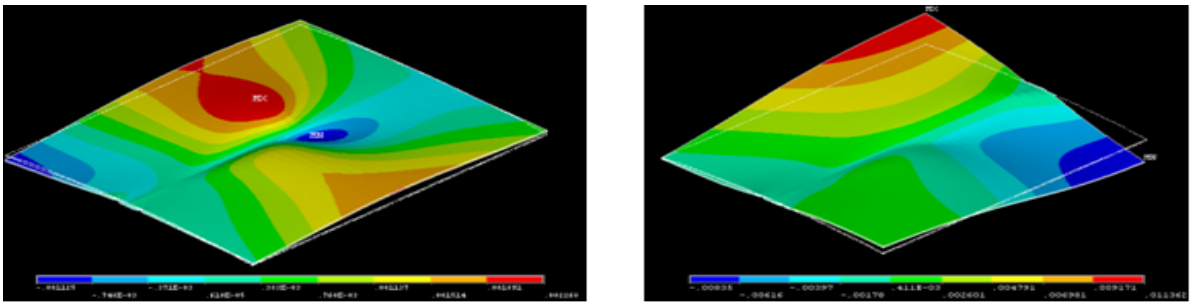

(a) The first buckling shape of welded shells in case 4.

(b) The second buckling shape of welded shells in case 4.

Fig. 7 Shape deformation of case 4 at the first global buckling and at the second global buckling.

Fig. 8 shows the distribution of longitudinal stress in midline of weldments after cooling down for cases 1, 4 and 5. Based on Fig. 8, in addition to case 5, other cases have asymmetrical stress pattern. The maximum and minimum values of tensile and compressive stress belong to case 1 with 79.04 total entropy and case 5 with 16.23 total entropy generation, respectively. Then, it can be calculated that mitigation technique of total entropy generation can minimize longitudinal stress and/ or radial deformation.

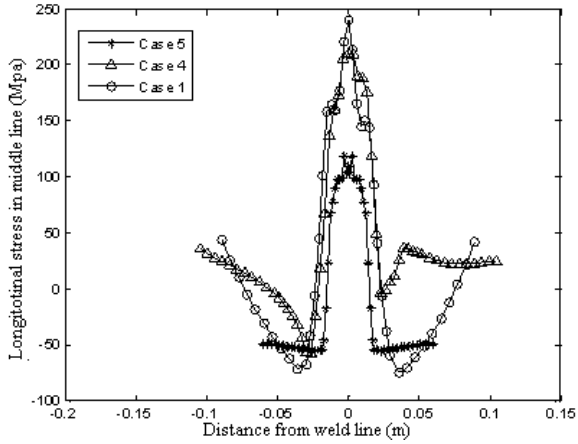

Fig. 8 Distribution of longitudinal stress for three different test cases

Fig. 9 reveals the effect of shell dimensions on time dependent pattern of entropy generation. As this Figure demonstrates, in the same weld length, increasing the span length of welded shells rises the maximum value of entropy generation. Similar conclusion can be drawn in weldments with the same span and different weld lengths. Also, in some cases, there is enough time to produce steady entropy generation. This behavior can be seen clearly in cases 1, 2 and 4. In case 3, generated entropy increases until torch removal and decreases after that. In the last case, after a short raising time, generated entropy decreases. The stage of steady state is not seen in these two last cases.

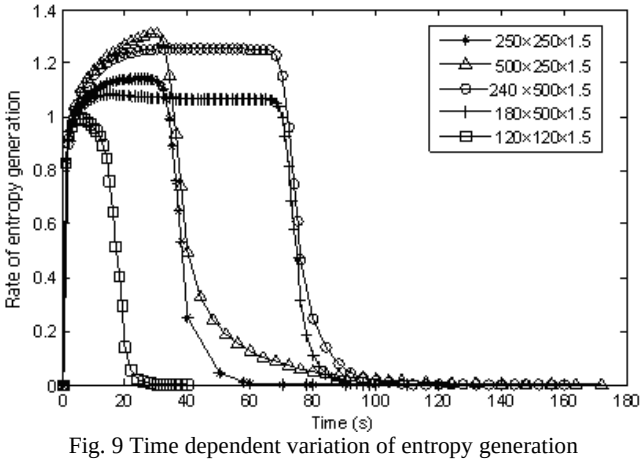

Fig. 9 Time dependent variation of entropy generation

The variation of total entropy generation with time is presented in Fig. 10. This Figure clearly shows linear variation of total entropy generation with time from starting to isothermal time. At isothermal time, the final value of total entropy generation is achieved. As it is expected, the differences between each two sequential values of the total entropy generation are almost equal.

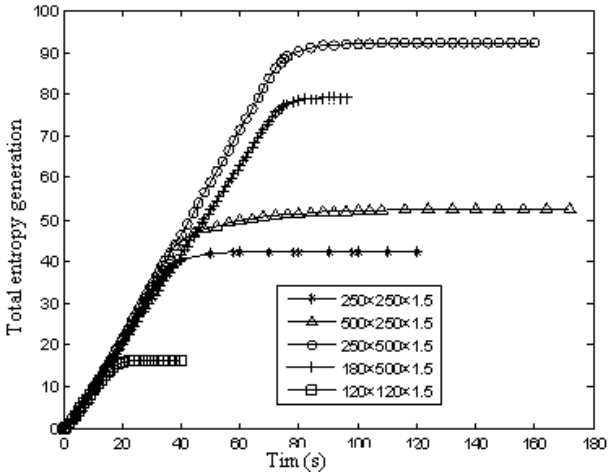

Fig.10: Variation of total entropy generation with time

Fig. 11 shows the variation of radial deformation versus total entropy generation which varies with time for each case.

Two middle points in the right and left sides of the weld line are selected to draw each part of Fig. 11. Based on this Figure, just before the first buckling, all cases experience small radial deformation with increasing the generated total entropy, but after that, radial deformation rises rapidly. Also, suddenly radial deformation change is occurred in some nodes but variation of total entropy is not significant at this time. This behavior is also seen at the time of second buckling.

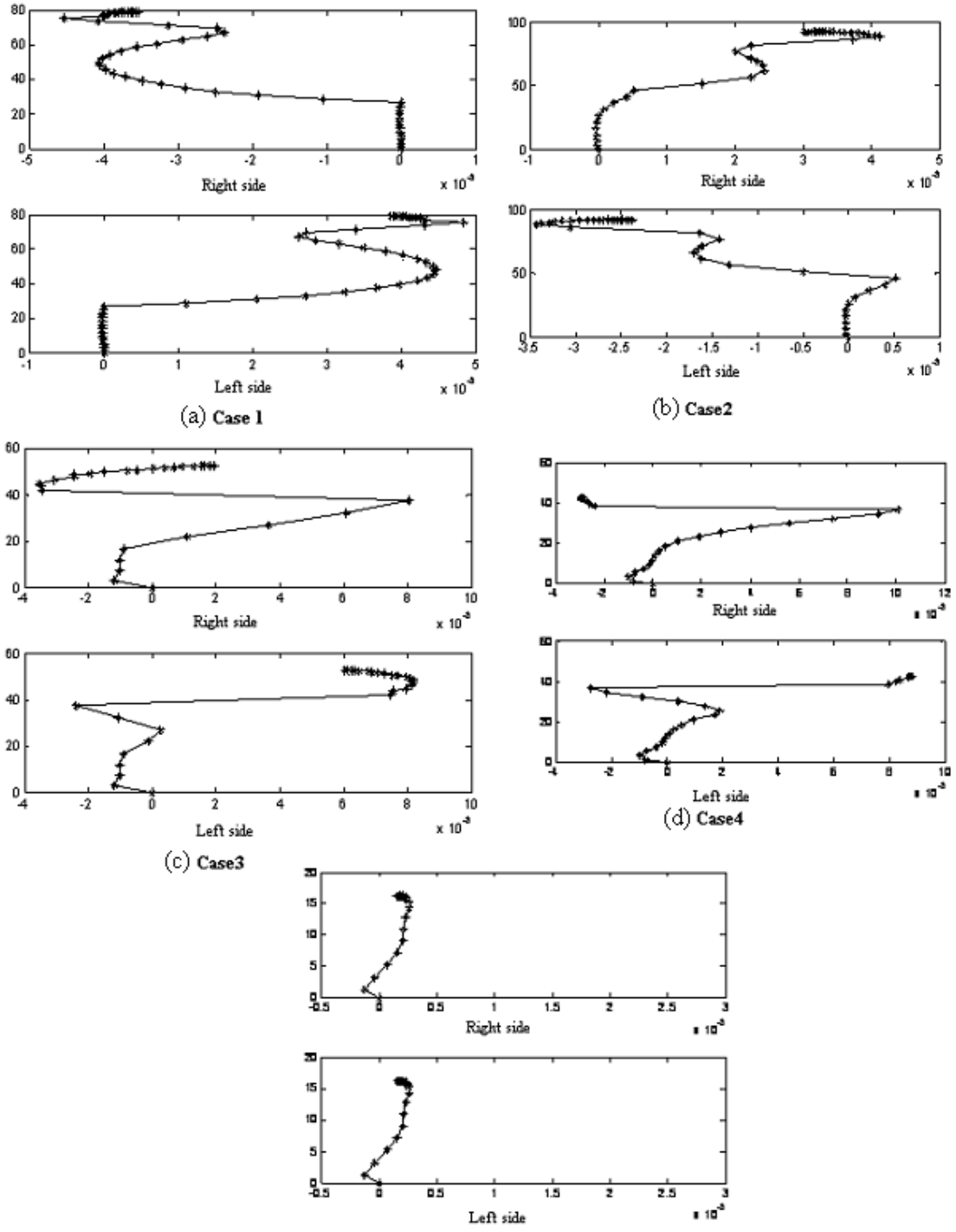

Fig. 11: Entropy- radial deformation for all cases

In Fig. 12, Entropy generation versus radial deformation is plotted for 3 different nodes on the left and the right edges of case 2. It can be seen that all nodes experience small radial deformation before buckling. However, middle and ending nodes have smaller deformation than the first nodes and it could be due to the sudden temperature variation in nodes which is produced by torch as soon as welding is started. Also, it is found that the first buckling affected first and middle nodes more than the last ones. But, after second buckling, the deformation rate of all nodes increases.

Sudden changes of deformation are not seen in case 5 because this case does not experience buckling during welding. Then sudden change of radial deformation and/ or increase the variation rate of out of plain deformation with small variation of entropy generation is a key to find

the buckling possibility of welded shell during the welding without employing eigenvalue analysis that is difficult and time consuming especially in post-buckling stage because of estimating transient longitudinal stress and equilibrium path at each time of loading step and applying them to eigenvalue analysis. Also, this plot can help to estimate the number of buckling that can be occurred during welding.

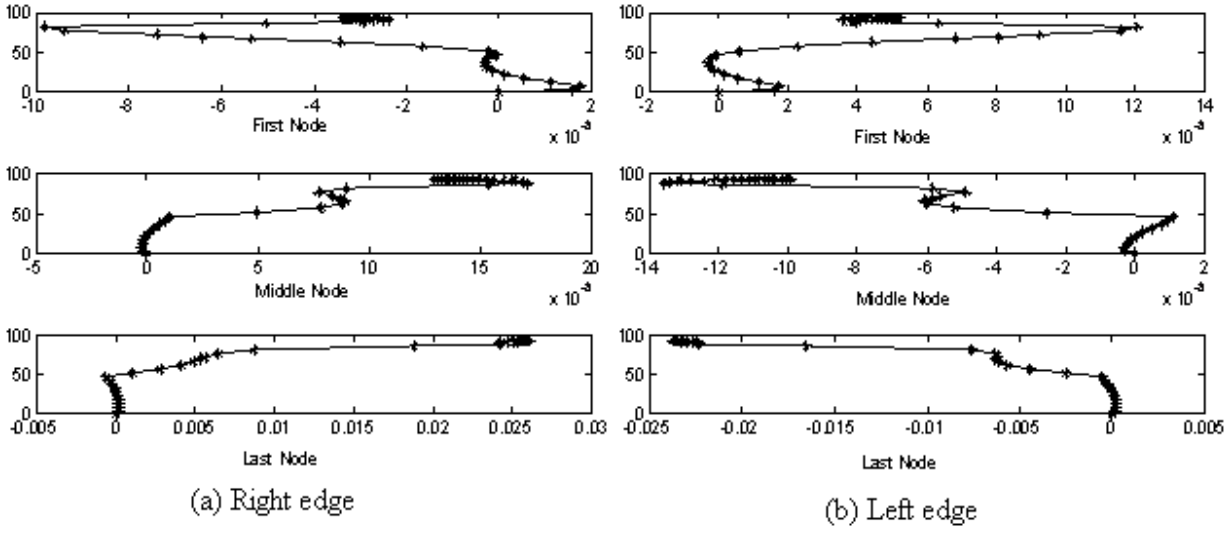

Fig. 12 Entropy generation versus radial deformation for different nodes in case 2.

REFERENCES

[1] Masubuchi K., Analysis of welded structures. Pergamon Press, Oxford, 1980

[2] Murakawa H., Ueda Y., Zhong X. M., "Buckling behavior of plates under idealized inherent strain," Transactions of JWRI, Vol.24, No.2,1995, pp.87-91.

[3] Michaleris P., Debiccari A., "Prediction of welding distortion," Welding Journal, Vol. 76, No. 4, 1997, pp. 172-180.

[4] Tsai C.L., Park S.C., Cheng W.T., "Welding distortion of a thin-plate panel structure," A.W.S., Welding Journal, Research Supplement, Vol. 78, 1999, pp. 156s-165s.

[5] Dean D., Hidekazu M., "FEM prediction of buckling distortion induced by welding in thin plate panel structures," Computational materials Science,Vol. 43, 2008, pp. 591-607.

[6] Michaleris P., Debiccari A., " A predictive technique for buckling analysis of thin section panels due to welding," Journal of Ship Production, Vol.12, No. 4, 1996, pp. 269-275.

[7] Michaleris P., Deo M.V., Sun J., "Prediction of buckling distortion of welded structures," Science and Technology of Welding & Joining, Vol. 8, No.1, 2003, pp. 55-61.

[8] Schenk T., Richardson I. M., Kraska M., Ohnimus S., "Modeling buckling distortion of DP600 overlap joints due to gas metal arc welding and the influence of the mesh density," www.sciendirect.com, Available online 30 May 2009

[9] Oddy A.S., Goldak J.A., McDill J.M.J., "Numerical analysis of transformation plasticity in 3D finite element analysis of welds," European Journal of Mechanics,A/Solids, Vol. 9, No. 3, 1990, pp. 253-263.

[10] Watt D.F., Coon L., Bibby M., Henwood C., "An algorithm for modeling microstructural development in weld heat affected zones (part a) reaction kinetics," Acta metal., Vol. 36, No.11, 1988, pp.3029-3035.

[11] Ziaee S., Kadivar M.H., Jafarpur K., "Experimental Evaluation of the Effect of External Restraint on Buckling behavior of Thin Welded Shells," IJST, Transaction B, Eng., Vol. 33,No.B5, 2009, pp.397-413.

[12] Fallahi A., Jafarpur Kh., and Nami M. R. "An investigation on thermal behavior of welded plates under the influences of essential thermal welding parameters," M.S. Thesis, Mechanical Eng., Shiraz, Iran, 2009.

[13] Ronda J., Oliver G.J., "Comparison of applicability of various thermo-viscoplastic constitutive models in modeling of welding," Comput. Methods Appl. Mech. Engrg., Vol. 153, 1998, pp.195-221.

[14] Brown S. B., Kim K. H., Anand L., "An Internal variable constitutive model for hot working of metals," International Journal of Plasticity, Vol. 5, 1989, pp. 95-130.